

Experimental analysis of a mechanical shear connector in concrete filled steel tube column

Análise experimental de um conector mecânico de cisalhamento em pilar misto de aço e concreto

J. G. R. NETO ^a
julianogeraldo.eng@gmail.com

A. M. SARMANHO ^b
arlene.sarmanho@gmail.com

Abstract

This work includes an analytical and experimental study of the structural behavior of shear connectors in composite columns, composed of concrete-filled circular hollow section. For this study was adopted a structural bolt like a shear connector in order to verify the validity of the analytical expressions in ABNT NBR 16239: 2014 [1]. Was carried out a series of push-out tests, fixing the outer diameter of the hollow section and varying the thickness, the bolt diameter, the strength of concrete and the hole dimension. Analysis of the results shows that is possible to use this type of shear connector. The Brazilian prescriptions results are conservative and may be adjusted to provide strength capacity value closest to the experiment.

Keywords: concrete filled steel tube, circular hollow section, push-out test.

Resumo

Este trabalho compreende um estudo analítico e experimental do comportamento estrutural de conectores de cisalhamento em pilares mistos, formados por perfis tubulares laminados de seção circular de aço preenchido por concreto simples. Para este estudo foi adotado um conector do tipo parafuso estrutural, a fim de verificar a validade das expressões analíticas constantes na ABNT NBR 16239:2014 [1]. Foi realizada uma série de ensaios experimentais de cisalhamento direto, fixando o diâmetro externo do tubo e variando a espessura, o diâmetro do parafuso, a resistência do concreto e a presença ou não de folga no furo. Da análise dos resultados observa-se que é viável a utilização desse tipo de conector, que as equações existentes para o dimensionamento dos mesmos estão a favor da segurança e podem ser ajustadas para fornecer valores de capacidade resistente mais próximo do experimental.

Palavras-chave: pilar misto preenchido, seção tubular circular, ensaio de cisalhamento direto.

^a Pontifical Catholic University of Goiás, School of Civil Engineering, Goiânia, GO, Brasil;

^b Federal University of Ouro Preto, Departament of Civil Engineering, Ouro Preto, MG, Brasil.

1. Introduction

Currently, an increase in the use of composite steel and concrete structures is observed, aiming to take advantage of the benefits of the combination of both materials. This association can be observed in the use of composite floor slabs with incorporated shaped steel, girder and composite columns, where it seeks to make the concrete resist to the compression tensions and to make the steel work under traction. Reduction of the construction time; reduction of the sections with consequent decrease of the own structure weight and increase of the pavement useful area; possibility to size de section so it can resist to the fire conditions; and better ductility and seismic resistance can be point out among 7.j0 the advantages to the use of composite columns.

According to ABNT NBR 8800:2008 [2]: Profile I of steel totally enveloped by concrete (Fig. 1-a); profile I of steel partially surrounded by concrete (Fig. 1-b); and steel tube with rectangular or circular section filled by concrete (Fig. 1-c and 1-d) can be mentioned among the usual types of composite columns.

The composite columns formed by steel tubes filled with concrete have advantages towards the simple elements, mainly in function of the increment of the structural properties due to the interaction between the tubular profile and the concrete core. Besides this, the confinement existing mainly in the circular sections increases the resistance of the

concrete due to the triaxial state of tensions, and the concrete complicates the occurrence of local buckling in the steel tube.

The simplified design method of composite columns introduced by the Brazilian rule [2] settles the following basic hypotheses for its validity: there is complete interaction between the steel and the concrete; the initial imperfections are consistent with those adopted to determine the resistant capacity of the steel beams submitted to the axial compression; and the local buckling for axial force and the bending moment cannot be of a last prevailing limit-state. To ensure the interaction between the two materials, the forces of shear developed in the interface steel-concrete must not exceed a value of resistance, natural or extended by the addition of mechanical connectors.

According to [3], the natural adherence can be divided into three distinct transfer mechanisms: adhesion (related to the chemical adherence between the concrete and the steel tube, - Figure 2-a -, it is developed in the initial stages of loading for small displacements and can be neglected for resistance effect); mechanical adherence (it results of the mechanical gearing between the concrete of the core and the superficial irregularities of the steel tube - Figure 2-b -, breaches in the initial loading stages due to the increase of the relative displacement between the materials); and friction (resistance portion that depends on the normal force applied in the interface and on the coefficient of friction - Figure 2-c - related to the degree of roughness of the steel surface and to the condition of the interface. For tubular sections filled with concrete, the rule [2]

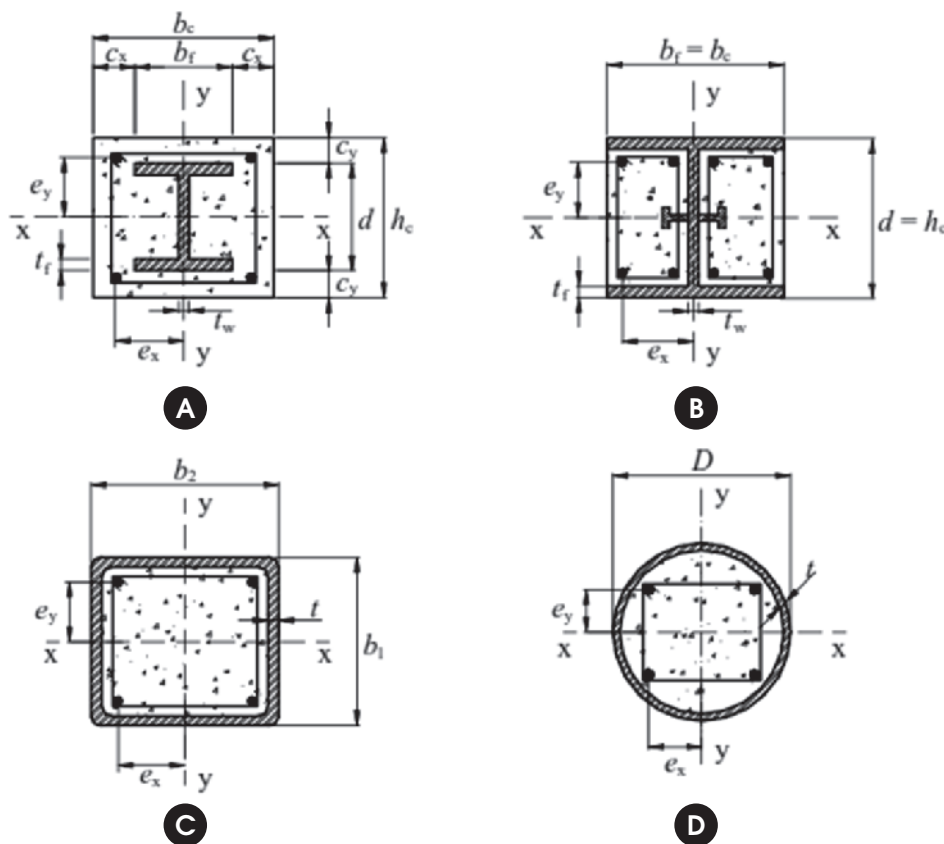


Figure 1
Types of cross-sections of composite columns. Source: (2)

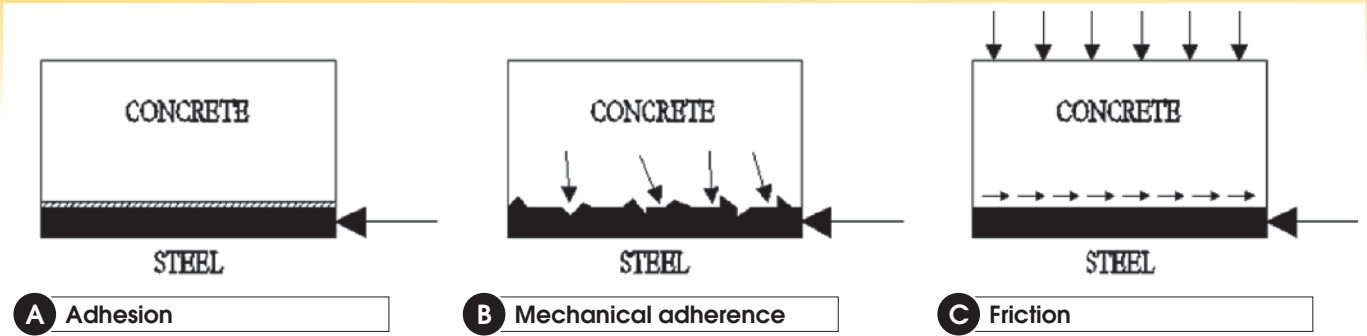


Figure 2 Idealized models of shear transfer in steel - concrete interface. Source: Adapted of (4)

specifies, as natural resistance to the shear, values of 0.4 and 0.55 MPa to rectangular and circular sections, respectively. For the adherence by adhesion in composite columns, [5] analyses the results of the experimental tests of 104 prototypes with circular tubes, 49 with rectangular tubes and medium D/t ratios between 15 and 35, which shows that the adherence tension: is larger for the filled columns of circular section than for the squares; do not have relation to the concrete resistance; reduces with the increase of the D/t ratio in function of the biggest influence of the retraction. With these results, it is suggested the expression to calculate the adherence tension between the concrete and the steel, given by the Equation (1):

$$f_{2\sigma} = 2,109 - 0,026 \cdot \frac{D}{t} \tag{1}$$

Where $f_{2\sigma}$ is the adherence tension in MPa; D is the external diameter of the tube in mm, and t is the tube thickness.

In the load introduction regions, which are those where localized variations of the requesting effort occur due to the beam-column connections, or in those where the interruption of the longitudinal reinforcement occurs, as in column redresses or basis connections, significant slip should be avoided in the interface between the two materials. Therefore, the length of the load introduction region represented by the parameter l_v , as showed in Figure 3, does not have to exceed two times the smaller dimension of the column section or one third of the distance between points of load introduction, being adopted the smaller of these two values. An average value for the shear tension transferred longitudinally in the interface can be obtained by the Equation (2):

$$\tau_{Sd} = \frac{N_{c,Sd}}{u_a \cdot l_v} \tag{2}$$

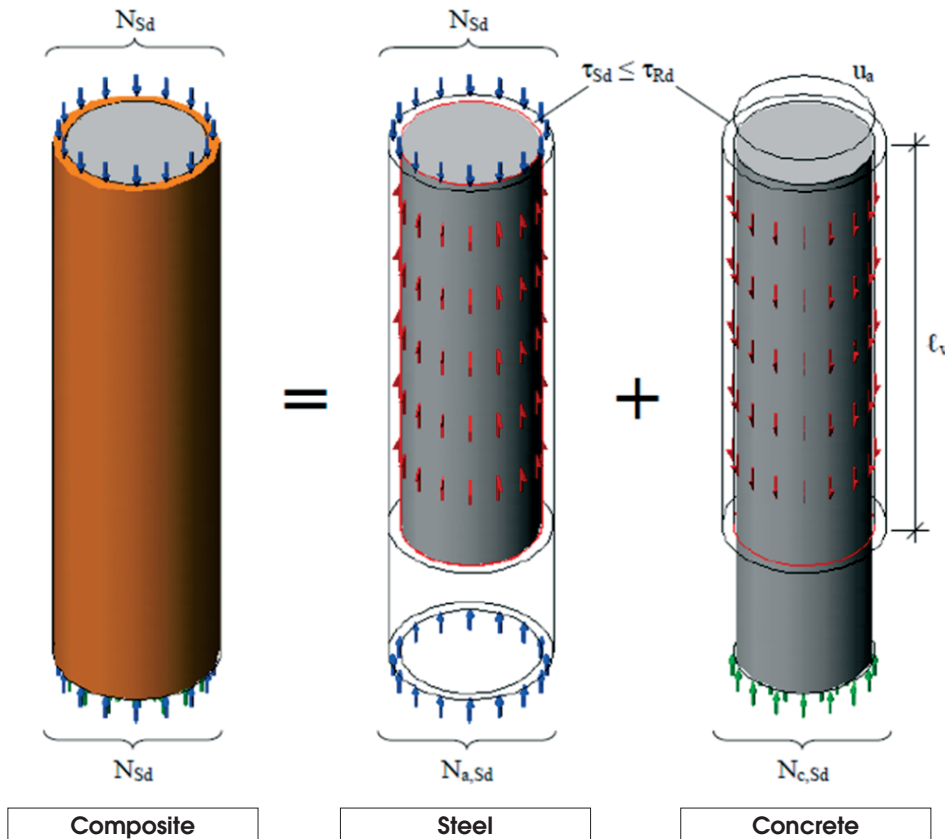
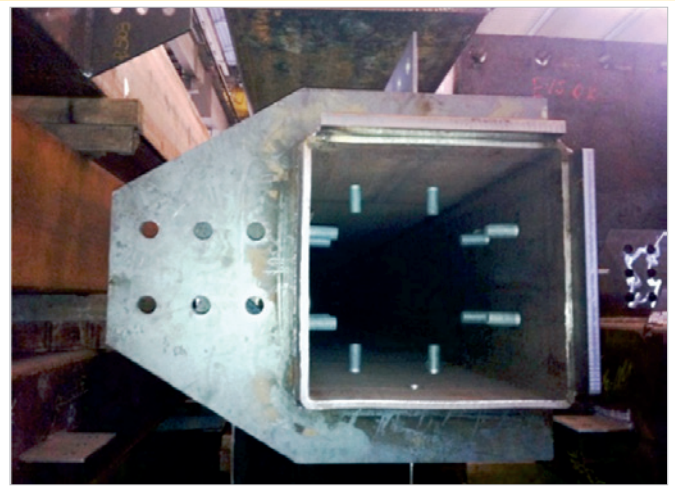


Figure 3 Components of loads and geometric properties to calculate the shear stress at the interface. Source: (4)



A Join with steel plate welded



B Internal detail of shear connector fixed in CFST

Figure 4

Example of application of load transfer device. Source: (6)

Where τ_{sd} is the shear tension of calculus; $N_{c,Sd}$ is the component of the normal force in the concrete; u_a is the transversal perimeter of the interface between steel and concrete; and l_v is the length of load transference.

When the shear tension of calculus τ_{sd} exceeds the resistant natural shear tension of calculus τ_{rd} , the use of additional mechanisms of load transference must be foreseen. A usual manner is the application of shear connectors, as it is illustrated in Figure 4. Some researches related to the behavior of shear connectors and load transference in the interface steel-concrete for composite elements are found in the literature. Among them, can be cited: [7], [8], [9], [10], [11] and [12], among others.

[13] performed a number of experimental tests of 71 models for analysis of the structural behavior and load transference in tubular composite col-

umns, without and with the use of mechanical connectors of shear. The connector used was the M16 bolt degree 5.6 with 65 mm of length, acting on three conditions of loaded introduction: only applied to the steel tube; only applied to the concrete; and applied to both simultaneously. From the analyses of the relative displacements and the measured strains in the two components, it was observed that the load transference between the two materials is better with the use of connector.

This work studies a shear connector of the structural bolt type, with the objective to verify the validity of the analytical expressions contained in the tubular structures norm [1] and to analyze its structural behavior. A number of experimental push out tests was performed, fixing the external diameter of the tube and varying the thickness, the diameter of the bolt, the concrete resistance and the presence or not of looseness in the hole.

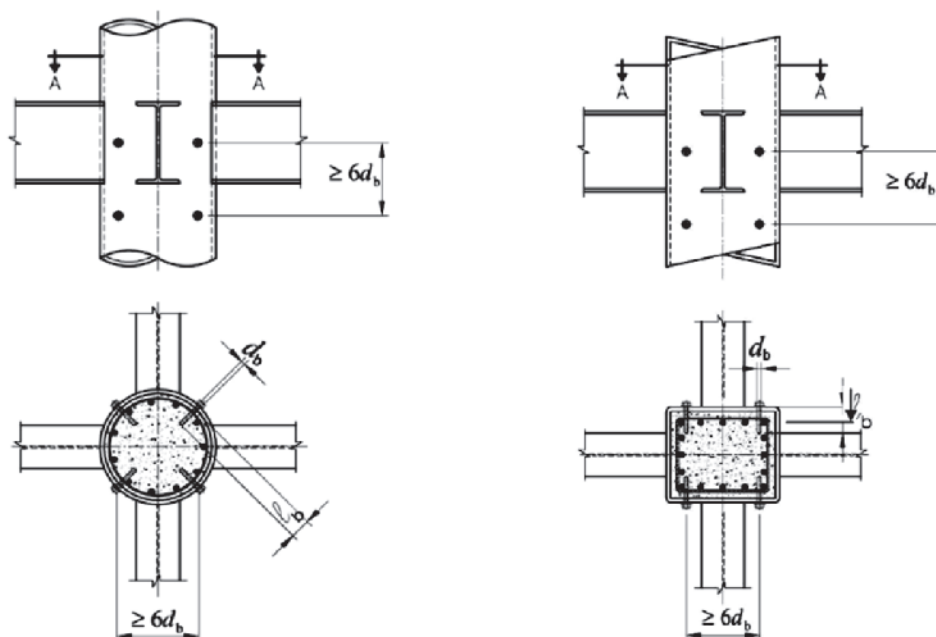


Figure 5

Device of load transfer type 1. Source: (1)

Table 1
Names and characteristic of experimental models of serie A

Name	Ø x t Tube (mm)	Ø Bolt (pol.)	Ø of Hole (pol.)	Kind of hole	f _{cm} (MPa)
C1-15,1-3/4-SF-21,7	219x15,1	3/4	3/4	SF	21,7
C2-15,1-3/4-SF-22,9	219x15,1	3/4	3/4	SF	22,9
C3-15,1-3/4-SF-30,8	219x15,1	3/4	3/4	SF	30,8
C4-15,1-3/4-SF-31,1	219x15,1	3/4	3/4	SF	31,1
C5-15,1-3/4-CF-31,1	219x15,1	3/4	13/16	CF	31,1
C6-15,1-3/4-CF-22,9	219x15,1	3/4	13/16	CF	22,9
C7-15,1-1/2-SF-26,0	219x15,1	1/2	1/2	SF	26,0
C8-15,1-1/2-SF-24,4	219x15,1	1/2	1/2	SF	24,4
C9-15,1-1/2-CF-22,7	219x15,1	1/2	9/16	CF	22,7
C10-8,2-3/4-SF-21,7	219x8,2	3/4	3/4	SF	21,7
C11-8,2-3/4-CF-21,6	219x8,2	3/4	13/16	CF	21,6
C12-8,2-3/4-CF-22,7	219x8,2	3/4	13/16	CF	22,7
C13-8,2-1/2-SF-21,7	219x8,2	1/2	1/2	SF	21,7
C14-8,2-1/2-CF-21,6	219x8,2	1/2	9/16	CF	21,6
C15-8,2-1/2-CF-21,6	219x8,2	1/2	9/16	CF	21,6

2. Analytical model

The norm [1] presents two types of special devices that can be used as shear connectors in the load introduction region for composite columns. The model that will be studied in this work is the type 1 device, where are used bolts (common or of high resistance) of which spacing between axes, in any direction, cannot be inferior to six times its diameter. The bolt head must be dotted with weld in the external side of the tubular profile to prevent its displacement during the concreting of the column. Figure 5 presents the referred device. The resistant force of calculus of each bolt is given by the lower obtained value of the Equations (3) and (4) presented below:

$$V_{Rd} = l_b d_b \sigma_{c,Rd} \leq 5 d_b^2 \sigma_{c,Rd} \tag{3}$$

$$V_{Rd} = 0,4\pi \frac{d_b^2 f_{ub}}{4 \gamma_{a2}} \leq 2,4 d_b t \frac{f_{ub}}{\gamma_{a2}} \tag{4}$$

Where l_b is the liquid length of the connecting bolt (deducting the thickness of the tube wall); d_b is the diameter of the connecting bolt; t is the thickness of the tube wall; f_u is the breaking strength from the steel of the tube; f_{ub} is the breaking strength of the connecting bolt; and $\sigma_{c,Rd}$ is the resistant tension of calculus of the concrete to the contact pressure, obtained by the Equation (5).

$$\sigma_{c,Rd} = \frac{f_{ck}}{\gamma_c \gamma_n} \sqrt{\frac{A_2}{A_1}} \leq f_{ck} \tag{5}$$

Where f_{ck} is the distinctive concrete resistance to the compression; A_2 is the loaded area; and A_1 is the support area, considering A_2/A_1 equal to 4.

3. Materials and experimental program

The experimental program was accomplished in the Structures Laboratory “Prof. Altamiro Tibiriçá Dias” of the Civil Engineer-

ing Department from the Federal University of Ouro Preto (UFOP), School of Mines. Two series of experimental push out tests were accomplished. In the series A, the external diameter of the tube was fixed and the thickness, the bolt diameter, the concrete resistance and the presence or absence of looseness in the puncture were varied. The series B was accomplished without the presence of shear connectors, in order to evaluate the natural adherence between the internal surface of the steel tube and the concrete core, besides the influence of the confinement.

3.1 Configuration of the prototypes

In series A, 15 experimental push out tests were accomplished using two sections of circular tubular steel profiles with diameter (D) of 219 mm and thicknesses (t) of 8.2 mm and 15.2 mm, in order to evaluate the influence of the D/t slenderness in the composite column behavior. All the bolts possess length of 4 “ (101.6 mm) and diameters of 1/2 “ (12.7 mm) and 3/4 “ (19 mm), being used a total of 4 units for each model. The total length of all the prototypes was of 1000 mm and two typologies of concrete f_{ck} were adopted, 20 and 30 MPa. Another evaluated factor was the influence that the puncture looseness, usually adopted in the manufacture process to facilitate the structure assembly, could have on the connector’s behavior. Thus, models with adjusted punctures had been confectioned, i.e., without looseness (SF), and others with looseness (CF) varying the type of drill used for the perforation.

Table 1 shows the nomenclature and the geometrical and mechanical characteristics of the prototypes. It is observed that the values of f_{cm} were obtained through characterization tests in the test day of each prototype. The models C11 and C14 did not had their results availed for analysis, due to problems that occurred during the execution of their tests.

The connectors were positioned at half height of the steel tube and organized symmetrically, as indicated in Figure 6-a. The head of all the bolts were welded in the external wall of the tube, to prevent

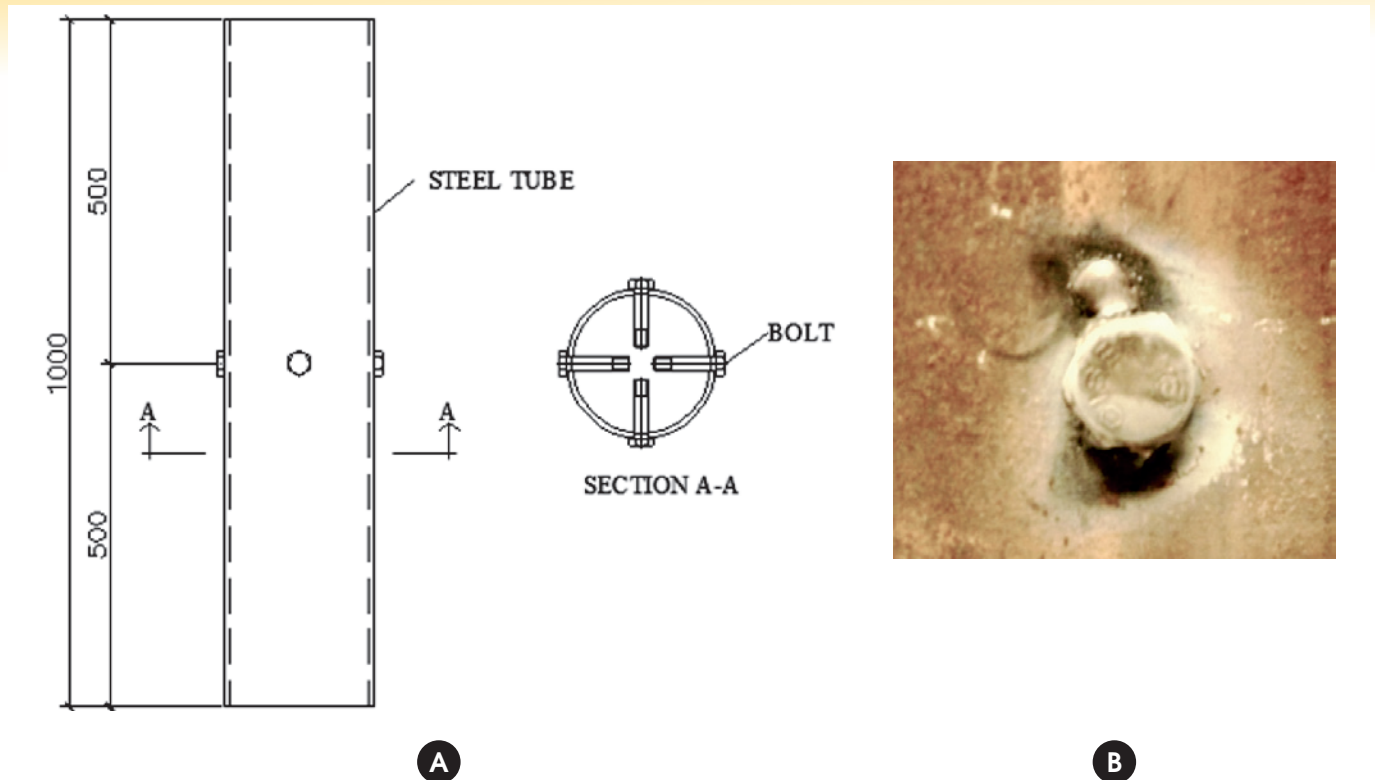


Figure 6
Position of bolts in the steel tube and welding darning detail of serie A

the displacement during the concreting and to assure the horizontality (see detail in Figure 6-b).

In series B, 4 experimental push out tests were accomplished using two sections of circular tubular steel profiles with diameter (D) of 219 mm and thicknesses (t) of 8.2 mm and 15.2 mm, without shear connector (SC), with total length also of 1000 mm. This series was tested in order to verify the behavior of the natural adherence tension between the internal wall of the steel tube and the filling concrete, in addition to evaluate the influence the D/t slenderness on its behavior.

The Table 2 shows the nomenclature and the geometrical and mechanical characteristics of the prototypes. It is observed that the values of f_{cm} are equal for all the pieces, since only one characterization of the concrete was accomplished, due to the prototypes that were tested during four consecutive days.

3.2 Concreting

The concreting of the series A models was accomplished in two stages, one for each type of concrete f_{ck} (20 and 30 MPa). Before the concreting, the pieces were cleaned internally. Figure 7-a shows the prototypes prepared for concreting and the Figure 7-b indicates an internal detail of the load transference mechanism. To get a startle region of concrete in the top of the column and a region of void in the root that could enable the relative displacement between the steel tube and the core of concrete, a ring of 50 mm was welded (see Figure 8-a), formed by the same profile of each model, in the top of the prototype. The pieces were concreted in inverted position of the test and on a wooden plate, so that a surface of leveled and smooth load application was obtained when the ring was removed. This way, a space of approximately 50 mm was left unfilled during the concreting, as is shown in Figure 8-b. This procedure was adopted in the concreting of the series A and B.

The concreting of the series B models followed the same procedure of the A series. However, a single stage was accomplished, since there was only one type of concrete f_{ck} (20 MPa).

3.3 Characterization of the steel

The structural tubes used were manufactured by the company Valourec & Mannesmann (V&M) Tubes do Brasil, which provided the results for the tests of mechanical characterization of the steel in Table 3. The steel used in the tubular profiles manufacture was VMB350 type (values of reference: $f_y \geq 350$ 485 MPa and $f_u \geq$ MPa, the 501 norm ASTM degree B).

The structural bolts were manufactured by the CISER company, which provided the results of the steel characterization tests presented in Table 4. The steel of the bolts was of the SAE J429 type ($f_u \geq 414$ MPa, dimensional norm ASME B18.2.1).

3.4 Instrumentation

All the prototypes of the series A were instrumented with two

Table 2
Names and characteristic of experimental models of serie B

Name	$\varnothing \times t$ Tube (mm)	\varnothing Bolt (pol.)	f_{cm} (MPa)
C16-15,1-SC-25,2	219x15,1	SC	25,2
C17-15,1-SC-25,2	219x15,1	SC	25,2
C18-8,2-SC-25,2	219x8,2	SC	25,2
C19-8,2-SC-25,2	219x8,2	SC	25,2



A



B

Figure 7
Preparation of models of the serie A to concreting



A



B

Figure 8
Details to obtain a gap of 50 mm in concrete

Table 3
Mechanical properties of steel of tubes

Ø x t Tube (mm)	f_y (MPa)	f_u (MPa)	Elongation (ΔL) (%)
219x8,2	385	582	33
219x15,1	384	598	41

Table 4
Mechanical properties of steel of bolts

Bolt Ø x l	f_{ub} (MPa)
1/2"x4"	660
3/4"x4"	665

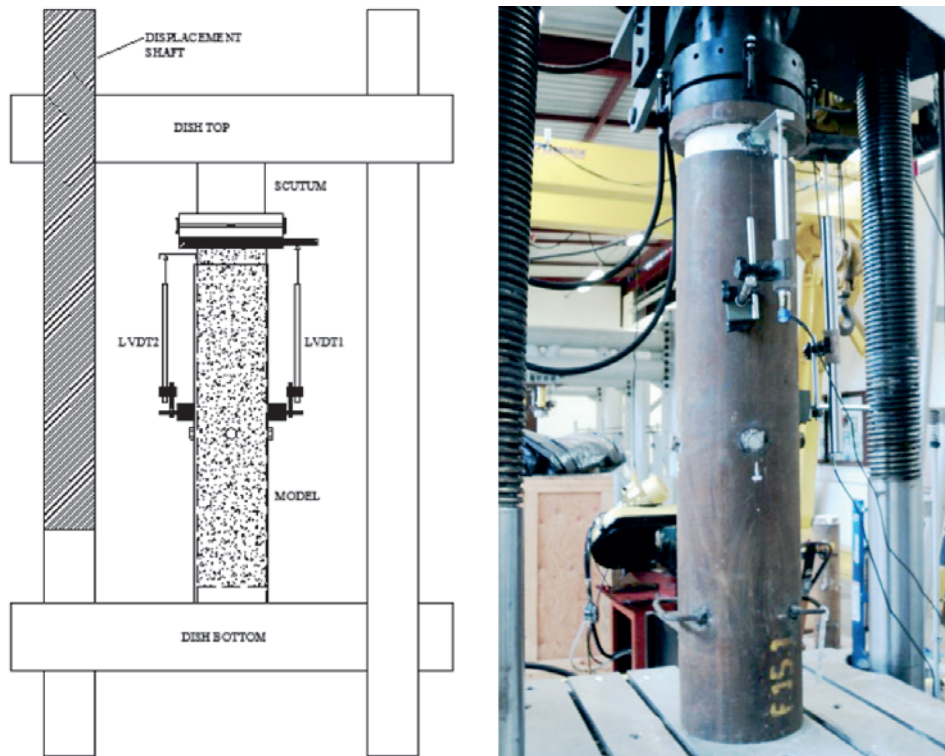


Figure 9
Representation of LVDT's position

linear displacement transducers (Linear Variable Displacement Transducer - LVDT) located on the top of the column, measuring the relative displacement between the steel tube and the concrete core (see Figure 9). The LVDTs were fixed in the external surface of the steel tube with the help of magnetic bases. To enable the

reading of the relative displacement between the steel tube and the concrete core, a rigid plate supported in the superior surface of the concrete region (between the prototype and the kneecap) and an angled connector fixed in the lateral of the concrete (to see detail in Figure 10) were used.

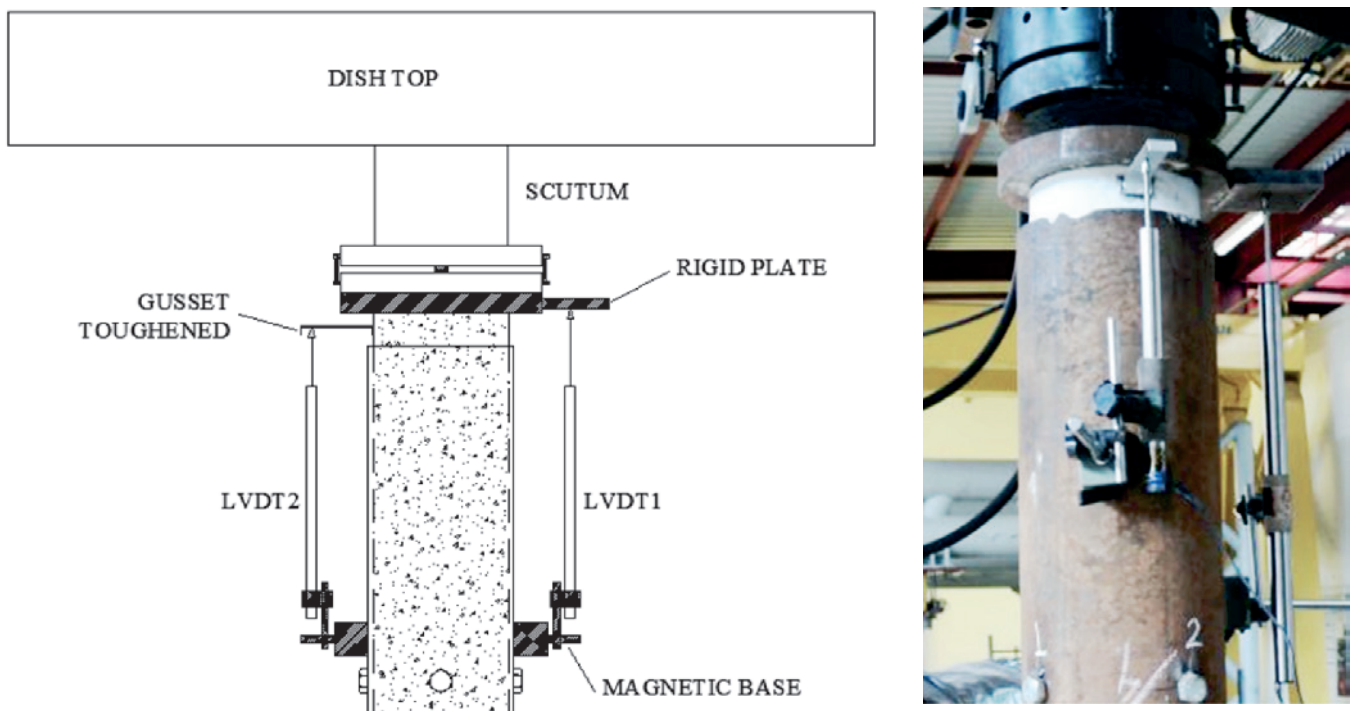


Figure 10
Detail of LVDT's position and accessories

Table 5
Distribution of models for each kind of extensometer adopted

Kind	Extensometer	Number	Models
1	Linear extensometer	5	C3,C4, C5 (serie A)
2	2 lines of rosettes de 90°	16	C13 (serie A)
3	1 lines of rosettes de 90°	8	C1,C10,C12,C15,C9 (serie A)
4	1 lines of rosettes de 90°	5	C16,C18 (serie B)

This measurement in two spots was fulfilled so that, having failure in the reading of one LVDT, the other could continue the measurements. Due to problems in the setting of the angled connector that appeared during the course of some tests, its results in the series A were discarded, without prejudice to the results obtained by the other LVDT. Yet, in series B, this system of additional measurement was not adopted.

The strain gauges was not same for all the prototypes, suffering changes of typology of electrical resistance strain gauge (EER) and of position, during the evolution of the tests. The first strain gauges typology adopted was with the use of linear strain gauges (KFG-5-120-C1-11 model). The other ones were adopted with the use of 90° rosettes (model KFG-2-D16-11), both of the KYOWA brand. Table 5 shows the models distribution for each one of the four typologies of strain gauges adopted, presenting the type of strain gauge and the quantity. The pieces that are not

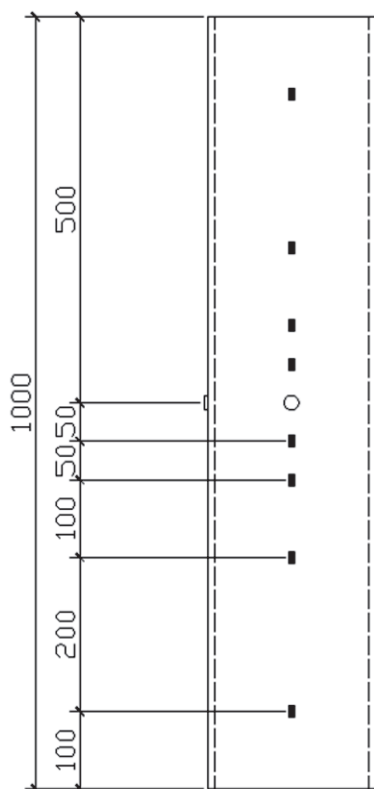
displayed in the table, did not receive strain gauges. Figure 11 illustrates the position of the strain gauges in the steel tube and the general instrumentation of the pieces.

3.5 Experimental procedure

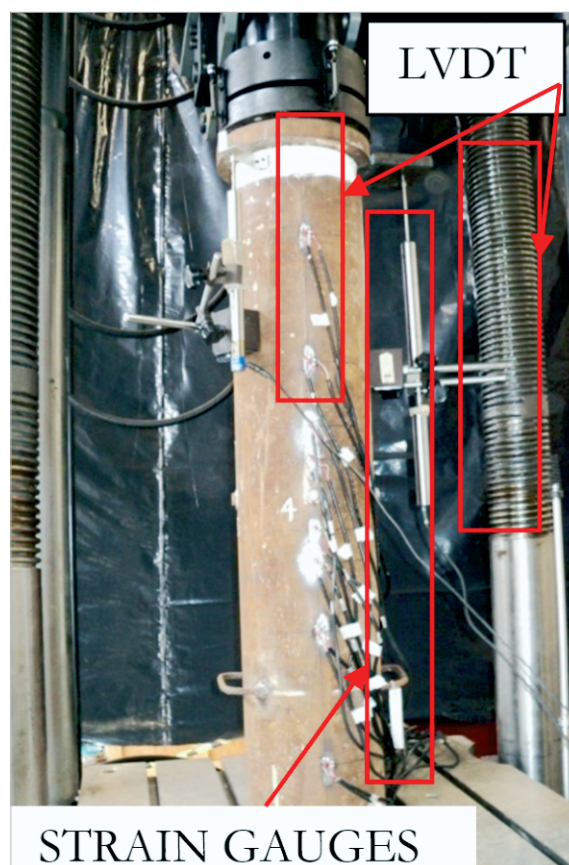
For the accomplishment of the tests, a serf hydraulic press HVL model of the SATEC series was used, manufactured by the company Instron with load cell with capacity of 2.000 kN.

The compression load was directly applied to the concrete core by displacement control. Once there was not a standard test procedure to be followed, an adaptation of the procedure specified by the Euro-code [14] was made for tests in shear connectors, as follows:

- The approach of the load application plate for all the stages was made by displacement control of 2 mm/min until reaching a load of 3 kN.



A Strain gages position



B Test setup and instrumentation of test specimen

Figure 11
Example of instrumentation models

- After this preload, the application of 5 load cycles and discharge of up to 40% of the waited theoretical load for the connectors, with load control of 10 kN/min.
- Finished the daily preload cycles, the models were continuously loaded by displacement control of 0.0025 mm/s until the end of the test.

The readings of loads and displacements of the LVDTs were accomplished by the data acquisition system connected to the test machine, controlled by the Instron Partner Software version 8.4a. The readings of the strain gauges were accomplished by the data acquisition system Spider 8, controlled by the HBM Catman Software version 4.5.

4. Results and discussions

4.1 Series A

The results of the prototypes C11 and C14 were discarded of this analysis, due to problems occurred during the execution of its tests. The Table 6 shows the values of the maximum forces applied to the extremity of the concrete core, compared with the following resistant capacities of the transversal sections: concrete by the simple compression ($A_c f_c$), concrete in confined state ($A_c \sigma_{c,Rd}$), yield ($A_a f_y$) and crushing of the steel tube ($A_a f_u$).

It is observed that the applied force overcomes the simple compressive strength of the concrete (relation (1)/(2)) from 1.68 to 3.19 times. This shows that the concrete is found in a multiaxial state of tensions, generated by the confinement effect of the concrete core through the walls of the steel tube, which extends its resistant capacity.

Analyzing the relation between the applied force and the resistant capacity of the confined concrete (relation (1)/(3)), it is verified that the values are between 1.18 and 2.24. This fact evinces that the consideration of the confinement effect leads to the results closer to the experimental ones. It can also be observed that the Equation (5), used to determine $\sigma_{c,Rd}$ leads to conservative values if com-

pared with the experimental ones.

Concerning to the resistance of the steel, it is observed that the relation between the operating load and the load of yield of the section (relation (4)) varies of 0.32 to the 0.81, and in relation to the crushing strength (relation (5)) varies of 0.21 to the 0.52. It can be evidenced that the steel tube presents a greater resistance, being working with values more conservatives in relation to the concrete core.

Table 7 presents the results of all series A tests, compared with the theoretical resistances evaluated for each failure mode considered by [1]. The values of theoretical ($V_{Rd,teo}$) and experimental resistance ($V_{Rd,exp}$) relate to a single connector, i.e., the load applied in the test was divided by four. The highlighted values refer to the limited dominant state for each prototype.

The experimental resistance was obtained from the first point of inflection of the load curves versus relative displacement, admitting that, in this point, the connector loses the admitted elastic-linear behavior for the project conditions. Similarly to what occurs in push out tests for evaluation of composite beams connectors [15], the results of identical models present significant variability that can be caused mainly by the form of concreting, densification and aggregates arrangement.

Of the values presented in Table 7, it can be observed that the dominant failure mechanism of the norm analytical expressions [1] is the crush of the concrete in the region of contact with the bolt. However, it is observed that the experimental values present a variation of 1.71 to the 6.11 times bigger that the theoretical. This indicates that the simplified analysis and isolation of failure mechanisms leads to resistant conservative capacity values. The experimental analysis suggests that there is an increase in the load capacity of the connector. This gain can be explained by the interaction between the collapse mechanisms, amplified by the confinement effect in concrete. In the columns C2 and C15 openings were made to observe the deformed configuration of the end connectors 3/4 "and 1/2 " respectively

Table 6

Comparison between applied force and resistant capabilities of steel and concrete

Model	Applied force (KN)	Concrete		Steel		Relation			
		Compression resistance (kN)	Confinement resistance (kN)	Yield resistance (kN)	Ultimate resistance (kN)	(1) / (2)	(1) / (3)	(1) / (4)	(1) / (5)
		$A_c f_c$	$A_c \sigma_{c,Rd}$	$A_a f_y$	$A_a f_u$				
(1)	(2)	(3)	(4)	(5)					
C1	1.940	608	868	3.714	5.629	3,19	2,24	0,52	0,34
C2	1.800	641	915	3.714	5.629	2,81	1,97	0,48	0,32
C3	1.894	862	1.232	3.714	5.629	2,20	1,54	0,51	0,34
C4	1.900	871	1.243	3.714	5.629	2,18	1,53	0,51	0,34
C5	1.889	871	1.243	3.714	5.629	2,17	1,52	0,51	0,34
C6	1.813	641	915	3.714	5.629	2,83	1,98	0,49	0,32
C7	1.375	728	1.039	3.714	5.629	1,89	1,32	0,37	0,24
C8	1.190	683	977	3.714	5.629	1,74	1,22	0,32	0,21
C9	1.925	636	907	3.714	5.629	3,03	2,12	0,52	0,34
C10	1.451	700	999	2.091	3.247	2,07	1,45	0,69	0,45
C12	1.699	732	1.045	2.091	3.247	2,32	1,63	0,81	0,52
C13	1.334	700	999	2.091	3.247	1,91	1,33	0,64	0,41
C15	1.171	696	996	2.091	3.247	1,68	1,18	0,56	0,36

Table 7
Comparison of resistance of shear connectors

Model	Concrete verification (kN)	Concrete verification (kN)	Shear of bolt (kN)	Crushing the tube wall (kN)	$V_{Rd,teo}$ (kN)	$VR_{d,exp}$ (kN)	$\frac{V_{Rd,exp}}{V_{Rd,teo}}$
	$l_b d_b \sigma_{c,Rd}$	$5d_b^2 \sigma_{c,Rd}$	$0,4\pi \frac{d_b^2 f_{ub}}{4 \gamma_{a2}}$	$2,4d_b t \frac{f_u}{\gamma_{a2}}$	(3)	(4)	(5)
C1-15.1-3/4-SF-21,7	51	56	76	413	51	163	3,18
C2-15.1-3/4-SF-22,9	54	59	76	413	54	191	3,55
C3-15.1-3/4-SF-30,8	73	80	76	413	73	124	1,71
C4-15.1-3/4-SF-31,1	73	81	76	413	73	133	1,81
C5-15.1-3/4-CF-31,1	73	81	76	413	73	140	1,91
C6-15.1-3/4-CF-22,9	54	59	76	413	54	171	3,18
C7-15.1-1/2-SF-26,0	41	30	33	275	30	125	4,17
C8-15.1-1/2-SF-24,4	38	28	33	275	28	133	4,72
C9-15.1-1/2-CF-22,7	36	26	33	275	26	160	6,11
C10-8.2-3/4-SF-21,7	55	56	76	218	55	95	1,72
C12-8.2-3/4-CF-22,7	58	59	76	218	58	98	1,69
C13-8.2-1/2-SF-21,7	37	25	33	146	25	105	4,20
C15-8.2-1/2-CF-21,6	37	25	33	146	25	88	3,51

(Figure 12-a and Figure 12-b). It can be observed in detail the bending of the bolt and the concrete shows no cracks around. Figure 12-c shows a detail of the shearing deformation at the interface region between the steel tube and the concrete to the model with connector 1/2 " , with visible stem vertical displacement relative to the bolt head.

Figure 13 shows the curves load versus relative displacement to all the prototypes of series A. The 6 mm offset value is highlighted as a reference to characterize the behavior and stiffness, according to the classification criterion [14].

A clear separation of the curves in two groups can be observed, the ones of 219x8.2 profiles with index of slenderness D/t of 26.7, and the ones of 219x15.1 with D/t of 14.5. It is verified, this way, that the tube slenderness influences in the load capacity and the ductility of the connector. The tubes with slenderness of 26.7 are more flexible and ductile than the ones of slenderness 14.5. It is observed that all the tubes with thickness 8.2 mm presented values of relative displacements well above 6 mm, while

some of the tubes of 15.1 mm present lower values and slightly superior others.

Analyzing Figure 14, that presents the load curves versus relative displacement only for the prototypes manufactured with 219x8.2 tube and concrete with fck of 20MPa, we can observe that the 3/4" connectors present a bigger rigidity and support more load than the ones of 1/2". The other prototypes have similar behavior.

To verify the influence of the puncture looseness in the structural behavior of the connector and in the resistance, Figure 15 Figure presents the curves of the C8 and C9 models, in the initial phase of the loading. It can be observed that the model with looseness (C9) presents a bigger relative displacement for the same load level than the model without looseness (C8) until a level of displacements of approximately 1.0 mm, value next to half the puncture looseness (0.8 mm, dashed line on the graph). Once after this two curves values meet and continue parallel, it can be concluded that the looseness is eliminated and the

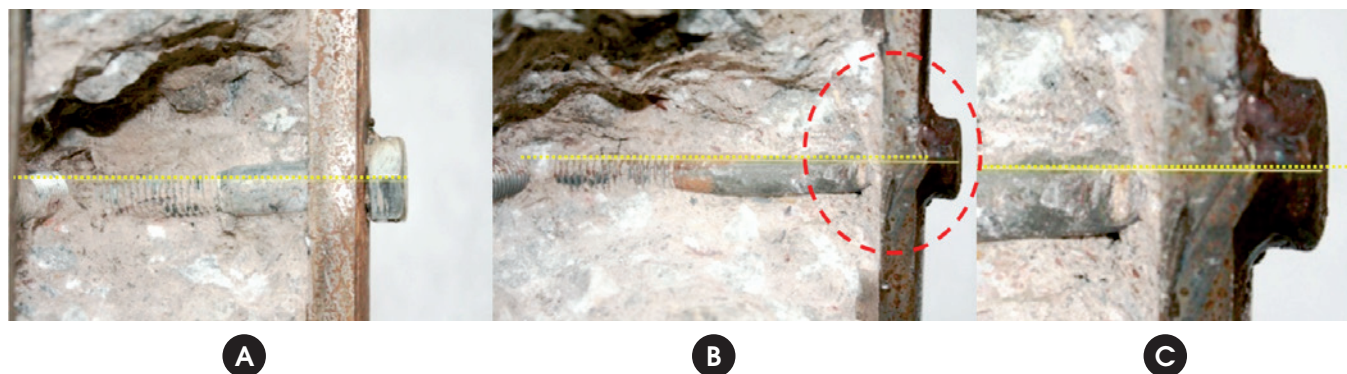


Figure 12
Deformed final configuration of the connectors: (a) Detail of connector of model C2; (b) Detail of connector of model C15; (c) Shear detail on connector of the model C15

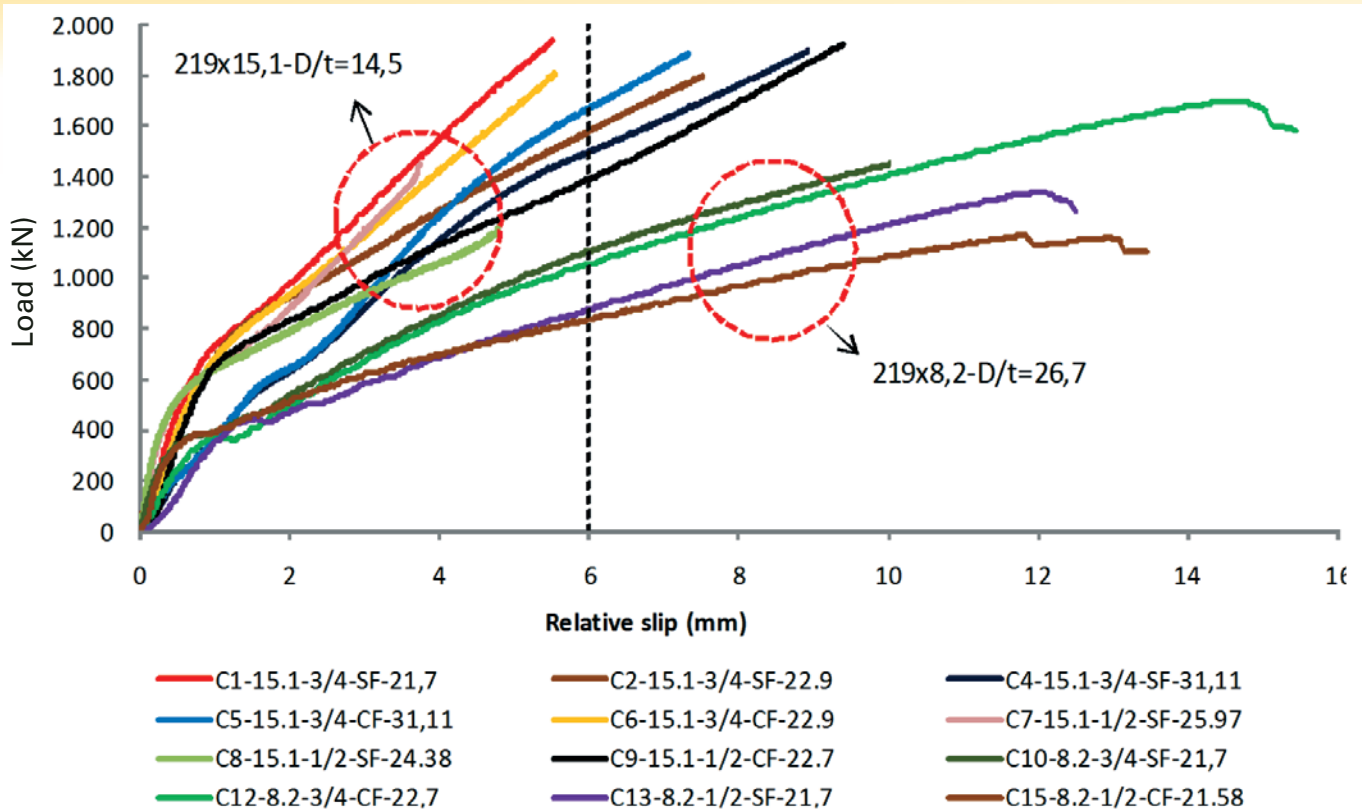


Figure 13
Overriding load curves versus displacement on the series A

columns now have the same structural behavior. Figure 16 presents the vertical and diametrical deformation curves measured along the tube length for prototype C1, 400 mm above and below the connectors' position (center) for different loading levels, varying from 10 to 100% of the maximum load applied. It is observed that, for the initial loading stages until 387 kN (20%), the deformations are approximately constant along the tube length, indicating that the load transfer between the concrete core and the tube wall is done in a gradual way through the natural adherence mechanisms. For the loading levels from 580 kN (30%), it is verified that the mechanic connectors start to be requested and to be part of the loading transfer system, due to the non-parallelism of the vertical deformations. For the diametrical deformations, it is observed the same effect

for the initial loading stages with large increases of deformations for the levels from 580 kN (30%) in the nearest region, below the connector. This fact evidences the emergence of the confinement tensions that tend to expand the tube diametrically.

4.2 Series B

This series was accomplished without the presence of shear connectors, in order to evaluate the natural adherence between the internal surface of the steel tube and the concrete core, besides the influence of the confinement. Figure 17 presents the overlay of the load curves versus relative displacement obtained for the four tested prototypes. The influence of the D/t slenderness is observed graphically in the tension of natural adherence, caused mainly by the action of the confinement effect. Table 8 presents the values of applied load and relative displacement, measured in the point of natural adherence loss between

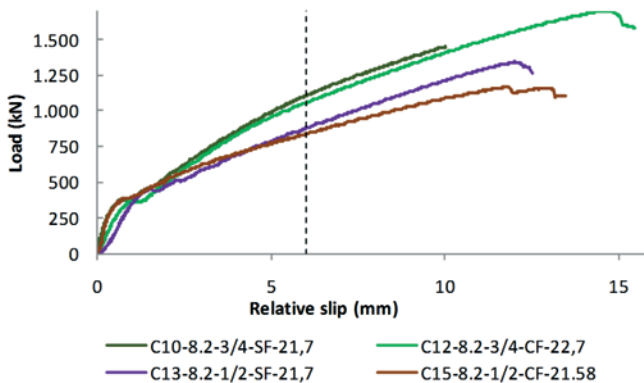


Figure 14
Curves load versus displacement relative for the tests with tubular section 219x8,2 mm e fck de 20 MPa

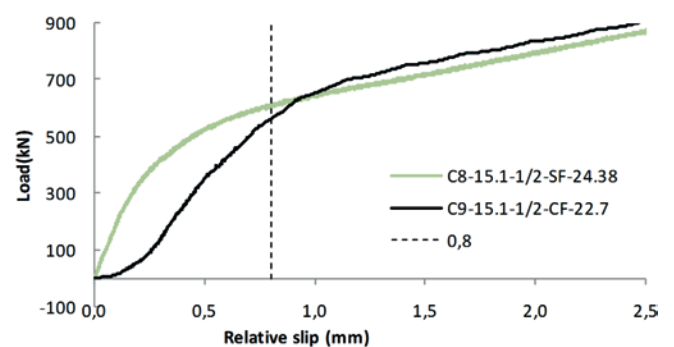


Figure 15
Curves load versus relative displacement - influence of the hole dimension for the C8 and C9 models

the concrete core and the steel tube, considered as being the first point of inflection of the curves.

Table 9 presents the values of the experimental adherence tension (τ_{exp}), calculated based on the Equation (2). A comparison with the value of reference (τ_{Rd}) established by the norm [2] for filled circular tubes and the value of $f_{2\sigma}$ proposed by [5], which is calculated by the Equation (1), is also done.

It can be observed that the relations between the tension of experimental adherence and the tension obtained by the Equation (1) ($\tau_{exp}/f_{2\sigma}$), for the C16 and C17 models (219x15.1), present values of 0.84 and 1.00 with average of 0.92. Yet, for the C18 and C19 models (219x8.2), these values are of 0.31 and 0.22 with average of 0.27. This indicates that, for sections with lower slenderness ($D/$

$t=14.5$), the proposal of the equation presents a good correlation with the experimental values. However, when it comes to sections with greater slenderness ($D/t=26.7$) the obtained values are over-estimated with relation to the ones obtained experimentally. This behavior can be observed in Figure 18Figure , which presents the curve $f_{2\sigma}$ versus D/t compared with the natural adherence tensions obtained from the tests.

When the experimental values are compared with the reference value (τ_{Rd}) equal to 0.55 MPa, it is observed that, for the C16 and C17 prototypes, the relations are of 2.66 and 3.14 with average of 2.9. Yet, for the C18 and C19 models, these values are of 0.80 and 0.56 with average of 0.68. Of these values, it can be verified that, for sections with lower slenderness ($D/t=14.5$) the experimen-

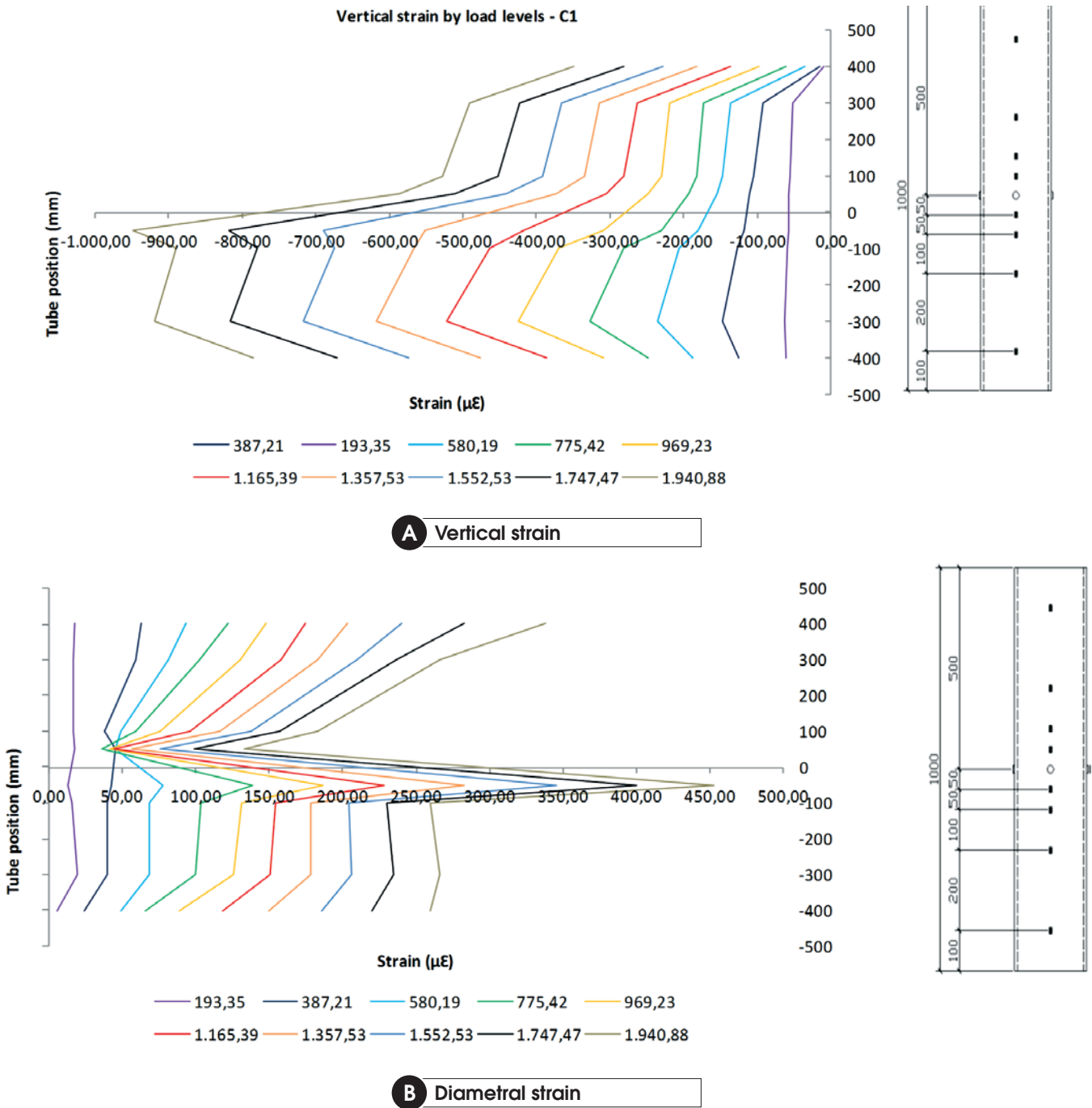


Figure 16 Distribution curves of the strains along the tube - C1-15.1-3/4-SF-21,7

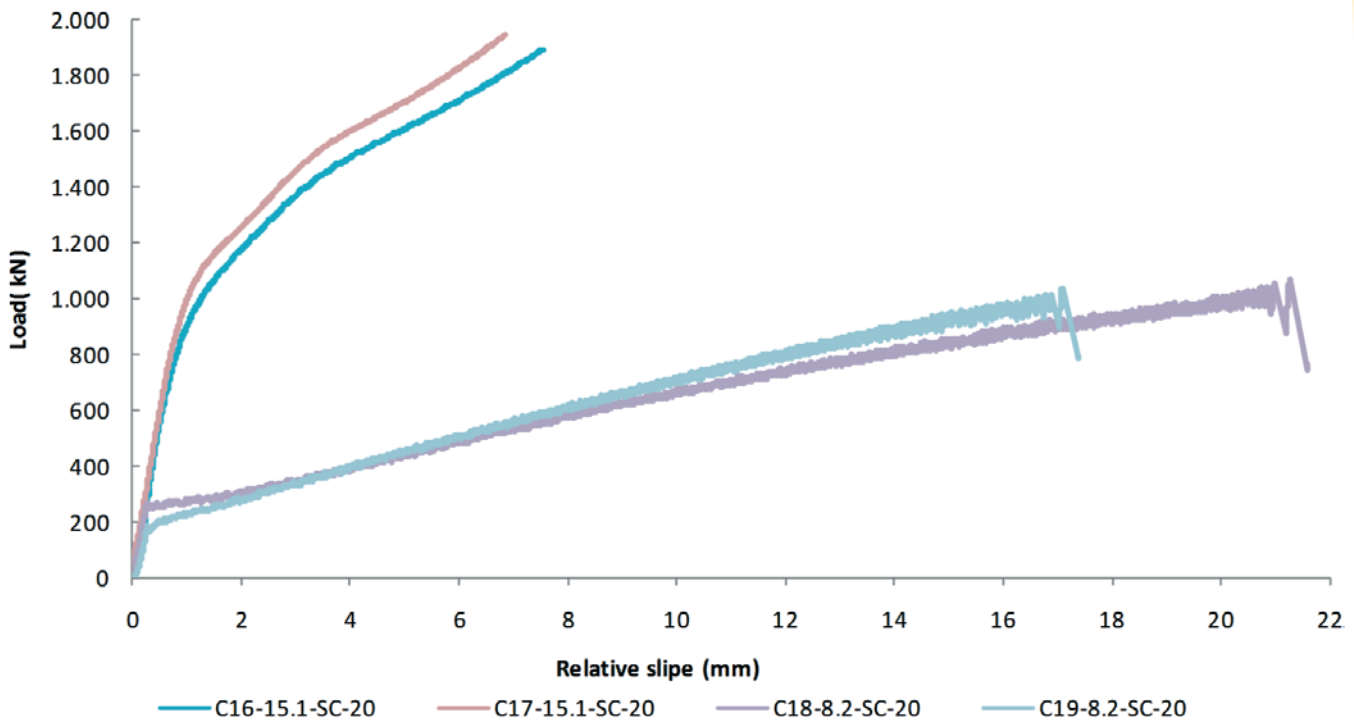


Figure 17
Curves load versus relative displacement series B

tal values are well superior to the normative referential. However, for sections with greater slenderness ($D/t=26.7$), these values are lower, being against the security for the conditions admitted in project situation.

Figure 19 presents the overlay of the load curves versus relative displacement for all the prototype confectioned with 219x8.2 tube of the series A and the B. The division of the curves in three groups, characterized by the absence of connector, and presence of 1/2 " and 3/4 " connectors, can be observed. It is verified that the presence of the connector influences in the load capacity of the prototype, increasing, as well, with the increase of the bolt diameter. It is observed that, for a same loading level, the relative displacements decrease with the presence and increase of de connector diameter.

Figure 20 presents the overlay of the load curves versus relative displacement for some of the confectioned prototypes with 219x15.1 tube of the series A, in order to facilitate the visualization, and the two of series B with relative displacement limited to 4 mm. It can be observed that the division of the curves into three groups characterized by the absence of connector, presence of 1/2" connectors and 3/4" connectors. Differently from

what was observed for the confectioned models with 219x8.2 tubes, it is verified that the presence and the increase of the connector diameter reduces the load capacity of the prototype. It is observed that, for a same loading level, the relative displacements increase with the presence and increase of de connector diameter. This behavior can indicate that, for sections with lower D/t slenderness where the natural adherence tension is enough to assure the total interaction between the

Table 8
Load applied and relative slip of loss of natural bond – série B

Model	Applied load (kN)	δ (mm)
C16-15,1-SC-25,2	823	0,86
C17-15,1-SC-25,2	974	1,10
C18-8,2-SC-25,2	266	0,32
C19-8,2-SC-25,2	185	0,28

Table 9
Experimental bond stress

Model	Applied load (kN)	τ_{exp} (MPa)	$f_{2\sigma}$ (MPa)	τ_{Rd} (MPa)	$\tau_{exp}/f_{2\sigma}$	τ_{exp}/τ_{Rd}
C16-15,1-SC-25,2	823	1,46	1,73	0,55	0,84	2,66
C17-15,1-SC-25,2	974	1,73	1,73	0,55	1,00	3,14
C18-8,2-SC-25,2	266	0,44	1,41	0,55	0,31	0,80
C19-8,2-SC-25,2	185	0,31	1,41	0,55	0,22	0,56

two materials, the utilization of shear connectors can reduce the resistance capacity of connection and increase the relative displacements. A possible reason for this is that the presence of the shear connectors introduces regions of tensions concentration in the interface between the steel and the concrete, which induce to a premature loss of the natural adherence tension between the two materials.

Figure 21 presents the distribution of vertical and diametrical tensions for the C16-15.1-SC-25.2 prototype. It is observed that, due to the absence of shear connector, the distribution of the vertical tensions (Figure 21-a) occur homogeneously along the tube length. In relation to the distributions of the diametrical tensions (Figure 21-b), it is verified that they occur homogeneously and approximately constant along the length, presenting a variation region close to the load application point. This behavior indicates that the low slenderness of the 219x15.1 section promotes a strong influence of the confinement in the composite column that, even

without shear connector, presents high rigidity and load capacity when compared with the 219x8.2 tube.

5. Conclusions

The analysis of the experimental results of push out tests (series A), aiming to the study of the structural behavior of bolts as mechanic shear connector in composite steel tubular column, demonstrates that the utilization of this type of element is viable. It can be observed, as well, that the results of the resistance obtained by the tests were above the obtained values by the expressions of resistance presented in the ABNT NBR 16239:2014. This way, it is verified that the equations are in favor of the security and can be adjusted to provide a value of resistance closer to the experimental.

From de analysis of the load curves versus relative displacement, it can be concluded that the bolts present a ductile and flexible behavior, being this a fundamental characteristic for its application as shear connector. The D/t slenderness of the tube influences in the rigidity and in the resistance of the connection, due to the increase of the concrete confinement tensions. The presence of looseness in the puncture exert influence in the rigidity of the connection, just in the initial stages of loading, not interfering in a significant way in the global behavior of the connector.

The distribution of the vertical and diametrical deformations along the tube wall confirms the efficiency of the mechanical connection mechanism in the transference of the shear efforts in the interface between the two materials, mainly for the prototypes with tube thickness of 8.2 mm that possess a lower natural adherence. It is also clear the presence of the confinement tensions that tend to expand the tube diametrically and increase the concrete resistance.

For the obtained results in series B, it is observed that the reference value of the natural adherence tension established by the ABNT NBR 8800:2008 is underestimated for the circular sections with low D/t slenderness, but overestimated for the lower thickness sections when compared with the experimental values. Such

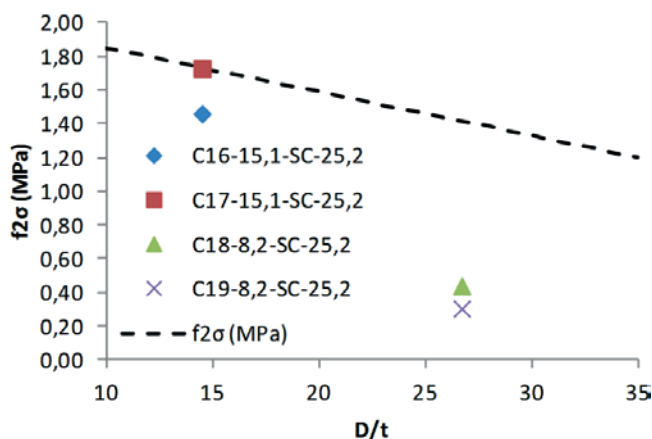


Figure 18
Comparison between curve $f_{2\sigma}$ in function of D/t ratio, and the variation of the experimental natural bond stress for the tested models

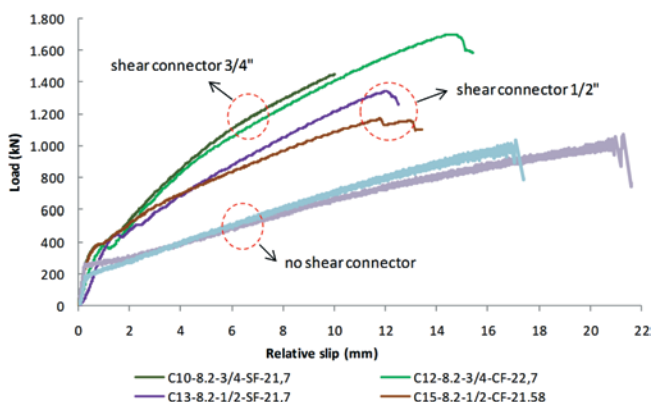


Figure 19
Comparison between the curves load versus displacement relative to the tube 219x8,2 of series A and B

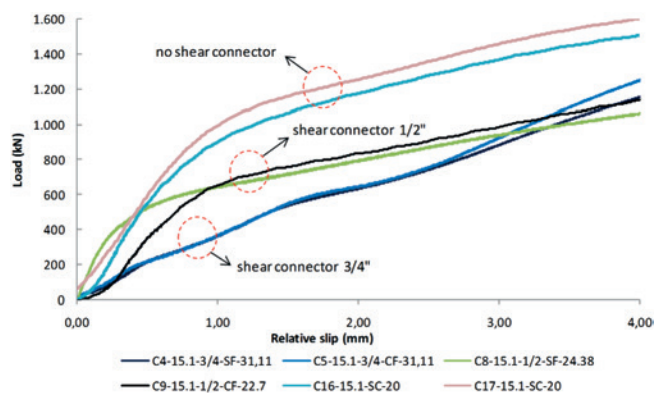


Figure 20
Comparison between the curves load versus displacement relative to the tube 219x15,1 of series A and B

behavior suggests that, for more slender sections, higher D/t relation, the normative prevision can be against the security. This indicates the necessity of more studies about the subject, as well as the development of analysis methodologies that consider the D/t relation in the determination of the natural adherence tension (τ_{Rd}), not restricted only to the section type (circular, rectangular, total or partially coated).

Making a comparison between the load curves versus relative displacement, the experimental results of the series A and B, grouped by the section of the analyzed tube, it was verified that, for the 219x8.2 tube, the shear connectors increased the capacity of the element and reduced the displacements. However, for the 219x15.1 tube, this behavior was contradictory, indicating that the presence of shear connectors in some cases can weaken the

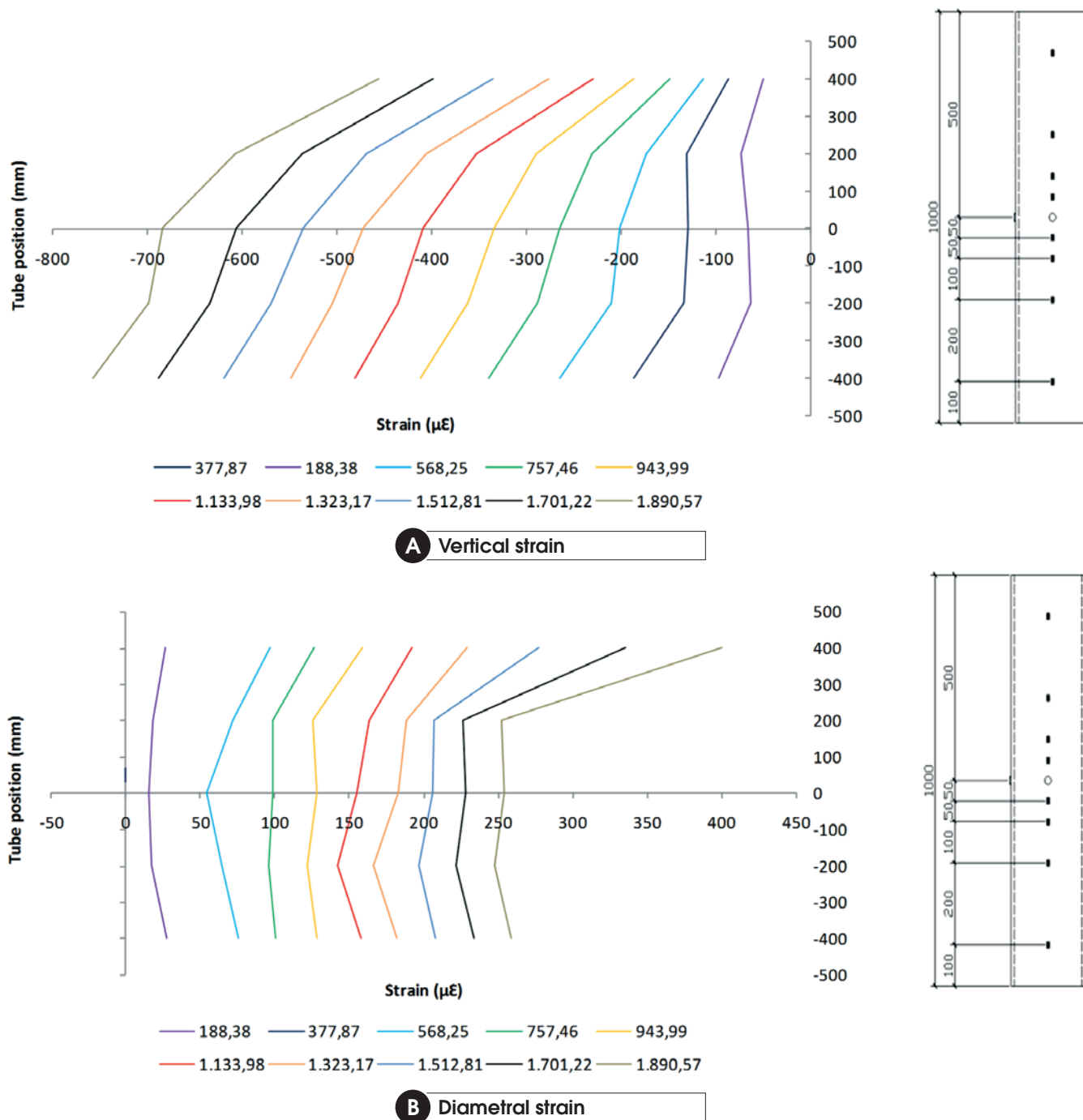


Figure 21
Distribution curves of the strains along the tube - C16-15,1-SC-25,2

connection between the steel interface and the concrete. This observation is not entirely conclusive, requiring further analysis.

6. Acknowledgements

The authors of this work acknowledge the furtherance organs CNPq, CAPES, FAPEMIG, and the company Vallourec & Mannesmann do Brasil. To PUC-GO and, principally, to UFOP for the logistical and financial support.

7. References

- [1] ASSOCIAÇÃO BRASILEIRA DE NORMAS TÉCNICAS. Projetos de estruturas de aço e de estruturas mistas de aço e concreto de edificações com perfis tubulares. - NBR 16239, Rio de Janeiro, 2014.
- [2] ASSOCIAÇÃO BRASILEIRA DE NORMAS TÉCNICAS. Projetos de estruturas de aço e de estruturas mistas de aço e concreto de edifícios. - NBR 8800, Rio de Janeiro, 2008.
- [3] OLIVEIRA, W. L. A. Análise teórico - experimental de pilares mistos preenchidos de seção circular, São Carlos, 2008, Tese (doutorado) - Escola de Engenharia de São Carlos, Universidade de São Paulo, 251 p.
- [4] JOHANSSON, M. Composite action in connection regions of concrete-filled steel tube columns. *Steel and composites Structures*, v. 3, n. 1, 2003.
- [5] ROEDER, C. W., CAMERON, B., BROWN, C. B. Composite action in concrete filled tubes. *Journal of Structural Engineering*, v. 125, n. 5, p. 477-484, 1999.
- [6] CODEME, E. Edifício para hotel. Guaratinguetá - SP, 2012.
- [7] VERÍSSIMO, G. S. Desenvolvimento de um conector de cisalhamento em chapa dentada para estruturas mistas de aço e concreto e estudo do seu comportamento. Belo Horizonte, 2007, Tese (doutorado) - Escola de Engenharia Civil, Universidade Federal de Minas Gerais, 316 p.
- [8] SIMÕES, R.. Efeito do confinamento em pilares mistos curtos de aço e concreto. Campinas, 2008, Dissertação (mestrado) - Faculdade de Engenharia Civil, Arquitetura e Urbanismo, Universidade Estadual de Campinas, 152 p.
- [9] NGUYEN, H. T. e KIM, S. E. Finite element modeling of push-out tests for large stud shear connectors. *Journal of Constructional Steel Research*, n. 6, p. 273-284, 2009.
- [10] JACOBS, W.P. e HAJJAR, J. F. Load transfer in composite constructions. ASCE 2010 Structures Congress, Orlando, Flórida, 2010.
- [11] BEZERRA, L. M.. Estudo Teórico Experimental da ligação entre pilares mistos preenchidos e vigas pré-moldadas de concreto. São Carlos, Tese (doutorado) - Escola de Engenharia de São Carlos, Universidade de São Paulo, 260 p.
- [12] ALMEIDA, P. H. F. Modelo numérico para um dispositivo de transferência de carga em pilares mistos tubulares preenchidos com concreto. Iberian Latin American Congress on Computational Methods in Engineering - CILAMCE, Ouro Preto, 2011.
- [13] STAROSSEK, U. e FALAH, N. The interaction of steel tube and concrete core in concrete-filled steel tube columns. *Tubular Structures XII*, London, 2011.
- [14] EUROPEAN COMMITTEE FOR STANDARDISATION. Design of composite steel and concrete structures. EURO-CODE 4, Brussels, 2001.
- [15] DAVID, D. L.. Análise teórica e experimental de conectores de cisalhamento e vigas mistas constituídas por perfis de aço formados a frio e laje de vigotas pré-moldadas. São Carlos, Tese (doutorado) - Escola de Engenharia de São Carlos, Universidade de São Paulo, 250 p.